Prediction of variability in wind turbine noise calculations

Benjamin Cotté, Yuan Tian

6th International Meeting
on
Wind Turbine Noise
Glasgow 20-23 April 2015

Prediction of variability in wind turbine noise calculations

Benjamin Cotté, Unité de Mécanique, ENSTA ParisTech, 828, boulevard des Maréchaux, 91762 Palaiseau Cedex, France, benjamin.cotte@ensta.fr

Yuan Tian, tian@ensta.fr

Summary

We propose in this work a method to predict the variability in wind turbine noise calculations due to wind speed and direction fluctuations. First, wind lidar data measurements during a 24-hour period are analyzed, and four periods with different atmospheric stability conditions are selected. Then, a wind turbine noise model based on Amiet's theory for trailing edge noise is presented and used to predict the sound pressure level at a fixed receiver during the 24-hour period. Finally, a Monte Carlo sampling method is described that allows us to accurately predict the statistics of sound pressure level during each selected period. The variability is seen to be much more pronounced during the day than during the night, and statistical quantities are shown to depend on the period duration considered.

1. Introduction

Wind turbine noise depends on numerous factors such as wind turbine characteristics, receiver position, atmospheric conditions, ground type and terrain features. The accurate modelling of all these factors is a difficult task. Furthermore, the accuracy of the models may be limited by uncertainties, that can be classified as either epistemic or aleatory. Epistemic (or reducible) uncertainty comes from incomplete information or imprecise measurement of a quantity (e.g. source-receiver geometry). On the other hand, aleatory (or irreducible) uncertainty, also called variability, is inherently random (e.g. atmospheric turbulence).

In this paper, we propose a method to predict the variability in wind turbine noise calculations due to atmospheric conditions. We consider a trailing edge noise model based on Amiet's theory, applied to a full-scale 2.3 MW wind turbine. Both wind speed and direction are considered random, and the variability of wind turbine noise is calculated using the Monte Carlo sampling method. To do so, high frequency wind lidar data measured at the SIRTA, an atmospheric observatory located South of Paris, are analyzed in order to obtain realistic probability density functions for different atmospheric conditions (stable and unstable atmospheres). Convergence and validation tests are performed to ensure the reliability of the method. Finally, predictions of the statistics of the sound pressure level for various periods are detailed.

2. Meteorological data measured at SIRTA

SIRTA (Site Instrumental de Recherche par Télédétection Atmosphérique) is an atmospheric observatory located 20 km south of Paris (Haeffelin *et al.*, 2005). In this work, we used data from two SIRTA instruments :

- a wind lidar that provides the wind speed and direction between 40-meter and 200-meter height with a time resolution of 4 seconds ;
- a sonic anemometer at 10-meters height that provides estimates of the friction velocity u*, temperature scale T* and Obukhov length L* every 10 minutes.

The parameters u*, T* and L* are useful to determine the type of stratification occurring in the atmospheric boundary layer (Stull, 1991). The atmosphere is typically stable (L* > 0) during a clear night, with temperature increasing with increasing altitude, which discourages vertical air motion. On the contrary, the atmosphere is typically unstable (L* < 0) during daytime, with significant vertical air motion.

We analyzed 24 hours of data between 8:30am the 19th and 8:30am the 20th of October 2011. This day was selected because no rain occurred, the cloud cover was low and the wind was mostly blowing from the West where the terrain is open and flat. In Figure 1, the wind speed U at 80-meter height and the angle τ are plotted for the whole 24-hour period, where τ is the difference between the wind direction at 80-meter height and its mean over the whole period. The mean wind speed is 6.7 m/s, and the mean wind direction is 296°, where 0° corresponds to the North ; by definition the mean of τ is 0° over the whole period.

We observe in Figure 1 than during the night - between approximately 6:54 pm and 8:17 am at this time of the year - the fluctuations of wind speed and direction are much weaker than during the day, which can be linked to the stability of the atmospheric boundary layer. Four periods of duration 40 to 60 minutes, noted by letters A to D in Figure 1, will be analyzed in more details in the following. During each period, the friction velocity u*, temperature scale T* and angle τ vary by a small amount. The corresponding mean meteorological quantities for these four selected periods are given in Table 1.

Table 1 : Mean meteorological quantities for the four selected periods.

Periods	<U> (m/s)	<τ> (°)	<u*> (m/s)	<T*> (K)	<L*> (m)
A : 10h15-11h05	6.4	-29	0.44	-0.16	[-98 , -79]
B : 13h55-14h35	7.7	-10	0.46	-0.08	[-280 , -128]
C : 19h05-20h05	7.5	+7	0.08	+0.05	[1.6 , 20]
D : 6h15-6h55	6.9	+19	0.18	+0.07	[21 , 47]

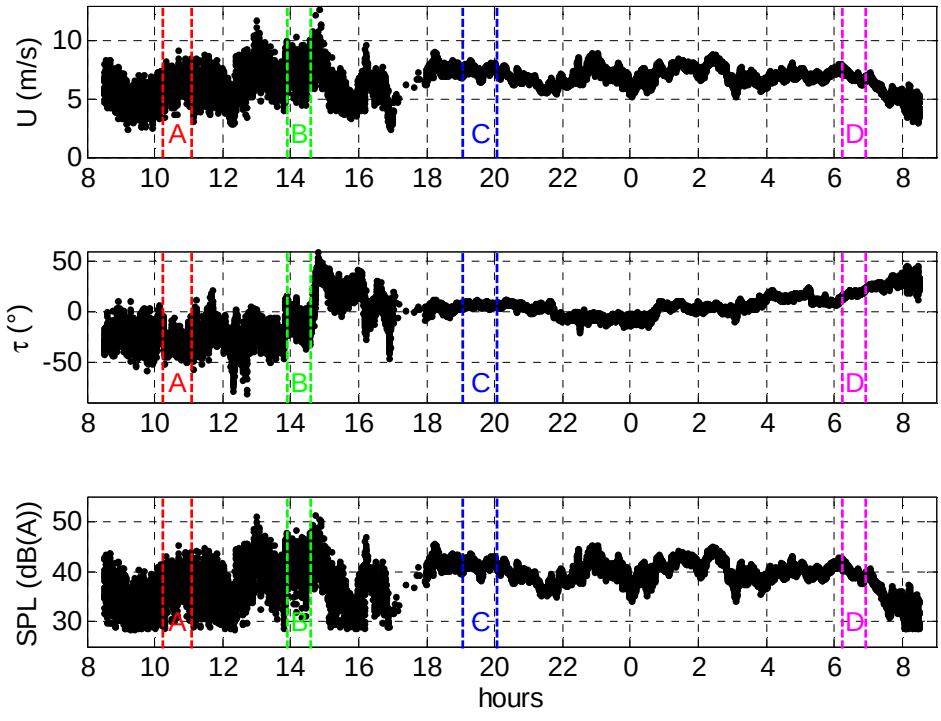

Figure 1: Wind speed U at 80-meter height, angle τ and calculated sound pressure level SPL.

3. Wind turbine noise calculations

3.1 Wind turbine noise model based on Amiet's theory

In a recent paper (Tian *et al.*, 2014), we showed that the trailing edge noise analytical model proposed by Amiet (1976) can be applied to a full-size wind turbine. The main difficulty of this model is to estimate the spectrum of wall pressure fluctuations at the trailing edge. Satisfying results were obtained considering the empirical model proposed by Rozenberg *et al.* (2012) that takes into account the effect of an adverse pressure gradient. Although other noise mechanisms such as turbulence inflow noise and separation noise may be important, we consider only trailing edge noise in this work.

This model is applied to a Siemens SWT 2.3-93 wind turbine of nominal power 2.3 MW. Its hub height is 80 meter, and it has three B45 blades of length 45 meters. In contrast with our previous work (Tian *et al.*, 2014), where wind shear were considered, we assume here that the wind speed is constant with altitude. This is usually a good approximation for unstable atmospheres, but not necessarily in stable atmospheres characterized by a stronger wind shear. The rotational speed is supposed to increase linearly from 6 rpm at the cut-in wind speed of 4 m/s to 16 rpm at the rated wind speed of 12 m/s, with a pitch angle equal to zero. The calculations are performed for a spectrum of 58 frequencies in order to estimate the third octave band spectrum between 50 Hz and 2500 Hz.

The receiver is fixed at a distance R = 200 meters from the wind turbine, and makes an angle τ with respect to the wind direction as shown in Figure 2 ; the rotor plane is always perpendicular to the wind direction. For the sake of simplicity, the receiver is placed on a ground that is supposed rigid, such that the sound pressure level (SPL) is 6 dB greater than the free field SPL. Note that it would be possible to consider a more realistic ground effect, as it is done in a companion paper (Tian and Cotté, 2015).

The third octave band spectrum of sound power level (SWL) in dB(A) estimated from the SPL at τ=0° (downwind) is plotted in Figure 3(a) for a wind speed of 4, 8 and 12 m/s. The peak of the spectrum is around 800 Hz for all wind speeds. The overall SWL is also plotted with respect to wind speed in Figure 3(b). Finally, the directivity of SPL normalized by its maximum and of amplitude modulation is plotted in Figure 4 for different wind speeds. Amplitude modulation AM is the difference between the maximum and minimum SPL during one blade rotation. When the SPL is maximum, for downwind and upwind directions, the AM is close to 0, while AM reaches a maximum of 6 to 8 dB(A) for crosswind directions, where the SPL is minimum. The directivities are very similar for the three wind speeds considered.

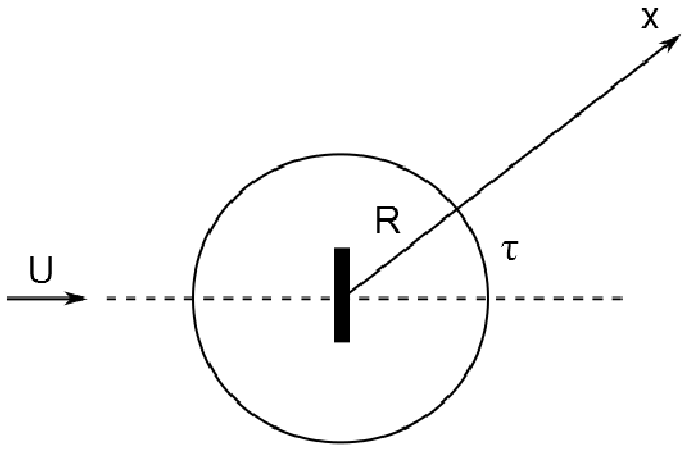

Figure 2: Angle τ between the wind direction and the direction of the receiver at distance R from the wind turbine.

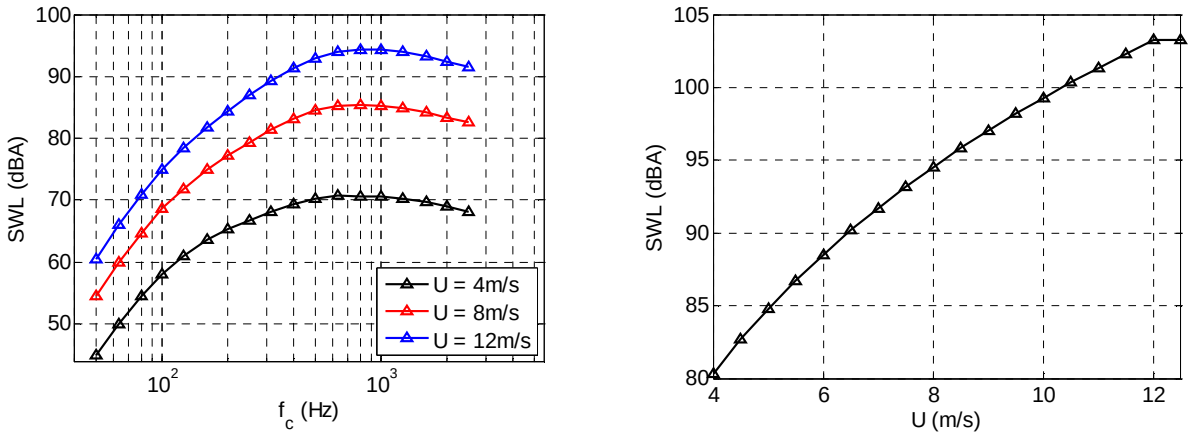

(a) (b)

Figure 3: (a) Third octave band spectrum of sound power level, and (b) overall sound power level with respect to wind speed U for τ=0° (downwind).

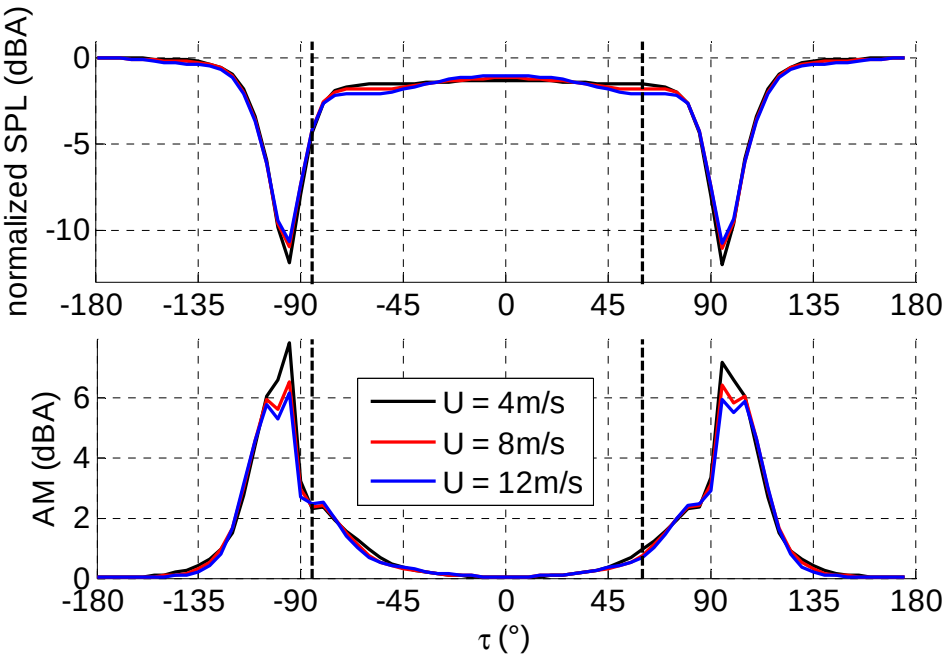

Figure 4: Directivity of the normalized SPL (top) and of amplitude modulation AM (bottom) for a wind speed of 4, 8 and 12 m/s.

3.2 Reference calculations using SIRTA meteorological data

The noise model is now used to calculate the overall SPL for each lidar measurement (U,τ) during the 24-hour period presented in Figure 1. First, the calculation is performed for each of the 20 459 measurement. This takes a long computation time since each calculation requires about 30'' to run on a regular PC. Second, the calculation is performed by linear interpolation between pre-calculated values. A total of 19 wind speed values between 4 and 13 m/s (step of 0.5 m/s) and 30 angular values for τ between -85° and 60° (step of 5°) are considered, which includes all the data plotted in Figure 1. The SPL values calculated by linear interpolation are in agreement with exact values within 0.1 dB, and are obtained almost immediately. Thus this interpolation technique will be used in the next section to predict SPL variability.

Figure 5 shows the SPL for all pre-calculated values. Because the angle τ is limited to the interval [-85° , 60°], the influence of the wind direction is quite weak. This τ interval is also delimited by the dashed vertical lines in Figure 4, which shows that AM will not exceed

2.5 dB(A) for this set of data. The SPL results for all measured data is shown in the bottom of Figure 1, where it is seen that the noise level fluctuations follow clearly the wind speed fluctuations.

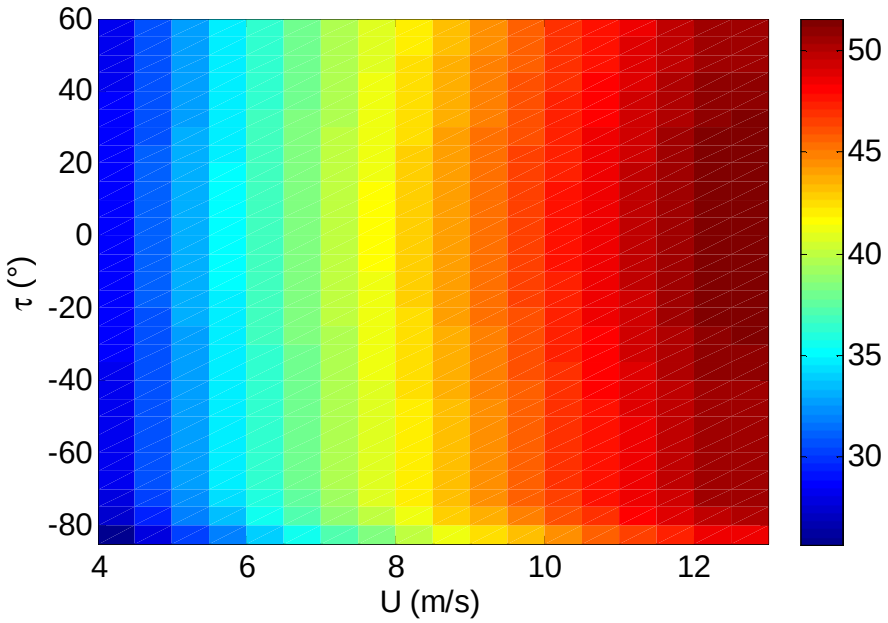

Figure 5: SPL as a function of wind speed U and angle τ for all pre-calculated values.

4. Prediction of wind turbine noise variability

4.1 Monte-Carlo method for predicting sound pressure level variability

We consider here a stochastic (Monte Carlo) sampling technique to predict the variability of the noise radiated by wind turbines. This technique is widely used and effective for uncertainty and sensitivity analysis (Helton *et al.*, 2006; Leroy *et al.*, 2010; Wilson *et al.*, 2014). Two random variables are taken into account, namely the wind speed U and the angle τ, characterized by their probability density functions (pdf) f(U) and g(τ). Thus the expected value of sound pressure level can be obtained by (Wilson *et al.*, 2014):

$$\langle SPL \rangle = \int_0^{+\infty} \int_0^{2\pi} SPL(U,\tau)\, f(U) g(\tau) dU d\tau \quad . \tag{1}$$

It is useful to introduce the cumulative distribution functions (cdf) F(U) and G(τ), that are the integral of the pdf f(U) and g(τ), to limit the integrals between 0 and 1. Since dF=f(U)dU and dG=g(τ)dτ, the integral becomes:

$$\langle SPL \rangle = \int_0^1 \int_0^1 SPL(U(F),\tau(G)) dF dG \quad . \tag{2}$$

For ordinary Monte Carlo sampling, N uncorrelated random pairs of values for F and G are generated in the interval [0,1], and the integral is approximated by the average of the integrand over these N pairs:

$$\langle SPL \rangle \approx \frac{1}{N} \sum_{n=1}^{N} SPL(U(F_n),\tau(G_n)) = \frac{1}{N} \sum_{n=1}^{N} SPL_n \quad . \tag{3}$$

Each SPL_n calculation is performed by linear interpolation using the method described in Section 3.2.

4.2 Estimation of probability density functions for wind speed and wind direction

To be able to apply the Monte Carlo sampling method to our problem, we first need to estimate the pdf of wind speed and direction from the meteorological data. For wind speed, we consider the normal and Weibull distributions, the latter being widely used in wind speed analysis (Lo Brano *et al.*, 2011). For the wind direction (angle τ), only the normal distribution is used.

The quality of the pdf fitting for the four selected periods is assessed using the Kolmogorov-Smirnov (K-S) statistical test (Lo Brano *et al.*, 2011). This test measures the distance of a random sample with a theoretical pdf by comparing the empirical cdf with the cdf of the reference distribution ; this distance is given by the K-S statistic D. Let the null hypothesis be that the samples are drawn from the reference distribution. The null hypothesis is rejected if the K-S statistic D is greater than a critical value that depends on the significance level α. The p-value is the probability of having a test statistic D as large or larger than observed, or otherly stated the probability that the empirical cdf is as far apart from the reference cdf. If p is smaller than α taken as 1% here, the null hypothesis is rejected.

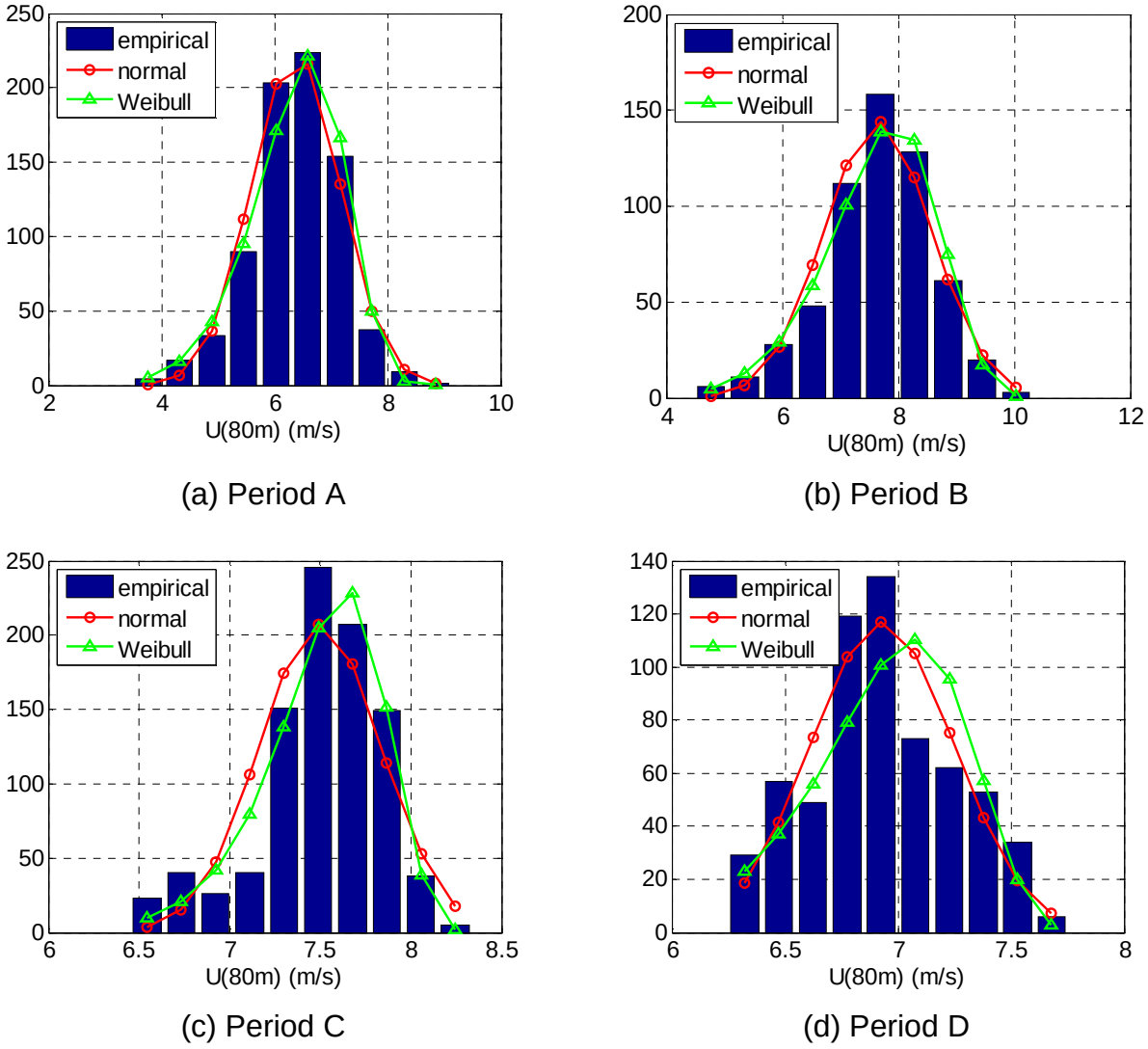

Figure 6 : Fitted wind speed probability density functions for the four selected periods estimated using 10 bins.

The results of the K-S test are summarized in Table 2, and associated pdf for wind speed are compared to the empirical pdf in Figure 6 using 10 bins. Table 2 shows that only two wind speed distributions are rejected (p < 1%), namely the normal distribution for period C and the Weibull distribution for period D. No normal distribution is rejected for wind direction. For period A, the Weibull distribution yields a better fit for wind speed than the normal distribution,

so it will be used in the next section. Both normal and Weibull distributions fit well the wind speed of period B. We choose arbitrarily to use the normal distribution in the Monte Carlo simulations of the next section.

Table 2 : Kolmogorov-Smirnov goodness of fit test with a significance level of 1% using a normal or Weibull distribution for the wind speed U and a normal distribution for angle τ. The bold values correspond to the distributions that are used for the Monte Carlo simulations.

Period	A	B	C	D
Time frame	10h15-11h05	13h55-14h35	19h05-20h05	6h15-6h55
p-value of K-S test for a normal distribution of U	9.6%	**12%**	5.5×10^{-5}	**1.9%**
p-value of K-S test for a Weibull distribution of U	**16%**	12%	**6.9%**	6.2×10^{-7}
p-value of K-S test for a normal distribution of τ	**21%**	**98%**	**16%**	**47%**

4.3 Results and discussion

In this Section, we will present results for the four periods selected in Section 2, using the distributions obtained in Section 4.2. To assess the quality of the results, we compare the statistics of the Monte Carlo simulations with the statistics of the reference data. More specifically, we look at the mean value <SPL>, the standard deviation σ(SPL), the median μ(SPL) and the interquartile range IQR(SPL). The standard deviation and the interquartile range are two different measures of variability. The standard deviation is useful when the distribution is normal; in this case 68% of the data are in the interval <SPL>±σ(SPL), and 95% of the data are in the interval <SPL>±2σ(SPL). The interquartile range is more general: it is the range of the middle 50% of the scores in a distribution. It is calculated as the difference between the 75th percentile and the 25th percentile.

First, we look at a typical convergence curve for the Monte Carlo simulations in Figure 7(a). The median and interquartile range of SPL is obtained using different number of simulations between 500 and 10 000. It is seen that the results do not vary anymore when the number of simulations is greater than 5000. In the following, N = 10 000 simulations are used for all Monte Carlo simulations. Second, the empirical cdf obtained from reference data and from Monte Carlo simulations are plotted in Figure 7(b) for the four periods. An overall good agreement is found between both curves, but small discrepancies are visible, especially for periods A and B corresponding to daytime. These cdf curves give us a lot of information about the probability of particular events. For instance, it appears that the probability of obtaining a sound pressure level greater than 45 dB(A) is significantly different from 0 only for period B.

The statistics for reference data and Monte Carlo simulations are given in Table 3, and also plotted as box plots in Figure 8. In the box plots, the central red line is the median, and the edges of the box are the 25th and 75th percentiles; thus the height of the box is the interquartile range. The whiskers extend to the most extreme data points not considered outliers; their length is 1.5 times the IQR. Outliers are plotted individually in red only for the reference data, since there would be too many outliers for the Monte Carlo simulations using N = 10 000.

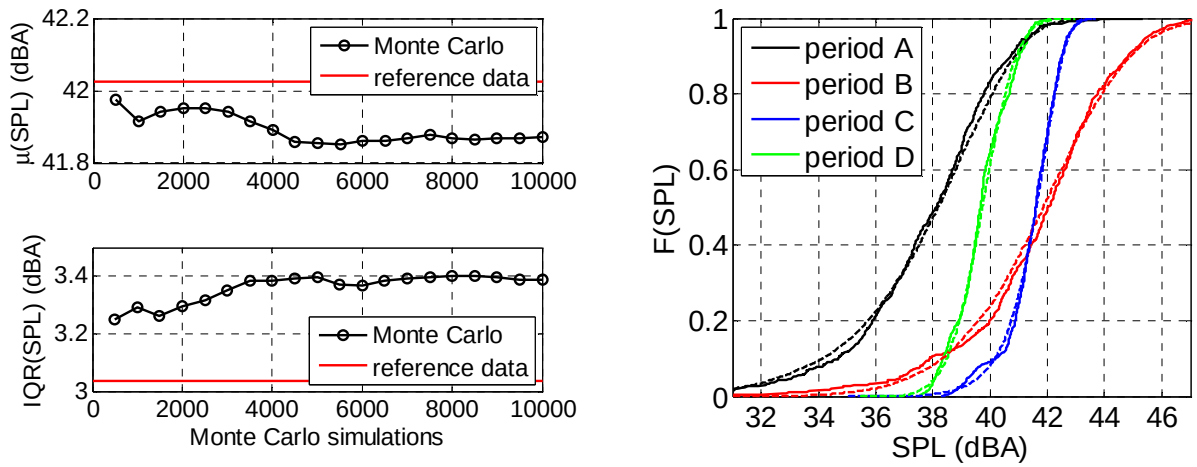

(a) (b)

Figure 7 : (a) Convergence of Monte Carlo simulations for median and IQR of SPL of period B, and (b) empirical cumulative distribution functions for the four periods obtained from the reference data (solid lines) and from Monte Carlo simulations with N = 10 000 (dashed lines).

Table 3 : Comparison of statistical quantities for SPL obtained from the reference data from Monte-Carlo simulations with N = 10 000.

Periods	Type of calculation	<SPL> (dBA)	μ(SPL) (dBA)	σ(SPL) (dBA)	IQR(SPL) (dBA)
A : 10h15-11h05	Reference	37.8	38.1	2.5	3.2
	Monte Carlo	37.8	38.2	2.7	3.5
B : 13h55-14h35	Reference	41.7	42.0	2.7	3.0
	Monte Carlo	41.7	41.9	2.6	3.4
C : 19h05-20h05	Reference	41.5	41.6	1.0	1.1
	Monte Carlo	41.5	41.6	1.0	1.2
D : 6h15-6h55	Reference	39.7	39.7	1.0	1.3
	Monte Carlo	39.7	39.7	1.0	1.3

We observe in Table 3 and Figure 8 that Monte Carlo simulations predict quite well the reference data statistics. The main discrepancies are for the IQR of periods A and B where a maximum difference of 0.4 dB(A) can occur. We note also that the measures of variability, σ(SPL) and IQR(SPL), are approximately three times larger during the 2 daytime periods the during the 2 night-time periods, as was already visible in the SPL plot of Figure 1.

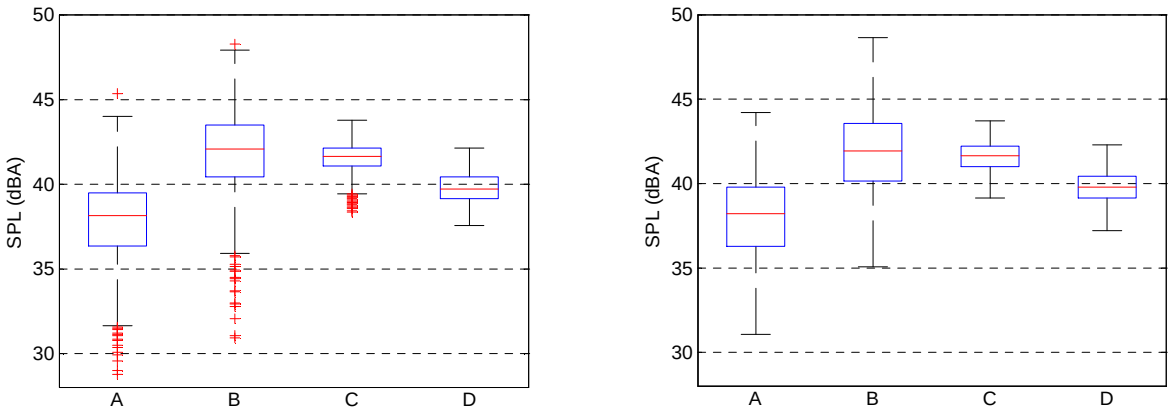

(a) (b)

Figure 8 : Box plots of SPL for the four selected periods using (a) reference data, and (b) Monte Carlo simulations with N =10 000. Outliers are shown only for reference data.

Finally, we look at the variability at an intermediate time scale of 10 minutes inside each interval. In Figure 9, the box plots for each 10-minute interval inside periods A and D are plotted using the reference data (similar results would be obtained using Monte Carlo simulations). The scale is different for both periods, extending over 18 dB(A) for period A and only 6 dB(A) for period D. It appears quite clearly that the SPL shows as much variability in all 10-minute intervals during the daytime period A, with an IQR between 2.7 dB(A) and 3.7 dB(A). The median value varies by a small amount, remaining between 37.4 dB(A) and 38.9 dB(A). On the contrary, the median value varies significantly during night-time period D, decreasing from 40.9 dB(A) in the first 10-minute interval to 38.5 dB(A) in the last one; the variability is small during this period, with the IQR remaining below 0.7 dB(A).

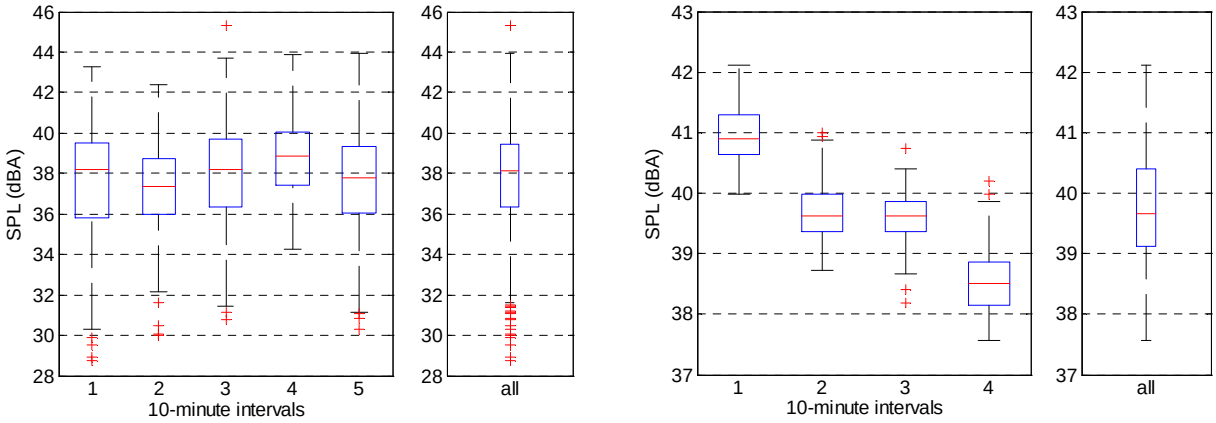

(a) (b)

Figure 9 : Box plots of SPL using reference data for each 10-minute interval of (a) period A, and (b) period D.

5. Conclusion

In this paper, we describe a Monte Carlo sampling method that can be use to predict wind turbine noise variability. The wind turbine noise model we use is based on Amiet's theory for trailing edge noise. From wind lidar data measured at SIRTA, we estimate the probability density functions of wind speed and direction during four selected periods, which allows us to predict the statistics of sound pressure level during these periods. The method is shown to yield accurate results by comparison with reference calculations. The variability is seen to be much more pronounced during the daytime periods than during the night-time periods, with an interquartile range approximately three times larger during the daytime periods. We also show that statistical quantities depend on the period duration considered. During night-time period D, the median value changes by more than 2 dB(A) between the four 10-minute intervals.

In this work, we use the ordinary or "brute-force" Monte-Carlo sampling method because we are able to obtain a good convergence in a small amount of computation time. For more computationally intensive models (e.g. with more random variables), it might be useful to use more advanced sampling strategies such as importance sampling or Latin hypercube sampling (Helton *et al.*, 2006; Wilson *et al.*, 2014). In the future, it could be interesting to account for the effect of wind shear (Tian *et al.*, 2014) and/or ground effect (Tian and Cotté, 2015) in the variability analysis.

Acknowledgements

The authors would like to thank David Ecotière from CEREMA, Fabrice Junker from EDF and Benoit Gauvreau from Ifsttar for useful discussions regarding uncertainty prediction methods.

References

Amiet R.K (1976) *Noise due to turbulent flow past a trailing edge,* Journal of Sound and Vibration 47(3), 387-393.

Haeffelin M. et al. (2005), *SIRTA, a ground-based atmospheric observatory for cloud and aerosol research*, Annales Geophysicae 23, 1-23.

Helton J.C., Johnson J.D., Sallaberry C.J. and Storlie C.B. (2006), *Survey of sampling-based methods for uncertainty and sensitivity analysis*, Reliability Engineering and System Safety 91, 1175-1209.

Leroy O., Gauvreau B., Junker F. and Bérengier M. (2010), Congrès Français d'Acoustique, Lyon, France, 12-16 April.

Lo Brano V., Oriolo A., Ciulla G. and Culotta S. (2011) *Quality of wind speed fitting distributions for the urban area of Palermo, Italy*, Renewable Energy 36, 1026-1039.

Rozenberg Y., Robert G. and Moreau S. (2012) *Wall-pressure spectral model including the adverse pressure gradient effects,* AIAA Journal 50(10).

Stull R.B. (1991) An Introduction to Boundary Layer Meteorology, Kluwer (Dordrecht).

Tian Y., Cotté B. and Chaigne A. (2014) *Wind turbine noise modeling : prediction of amplitude modulation and influence of atmospheric conditions*, Forum Acusticum, Krakow, Poland, 7-12 September.

Tian Y. and Cotté B. (2015) *Modelling of ground and atmospheric effects on wind turbine noise*, 6th Wind Turbine Noise Conference, Glasgow, UK, 20-23 April.

Wilson D.K., Pettit C.L., Ostashev V.E. and Vecherin S.N. (2014), *Description and quantification of uncertainty in outdoor sound propagation calculations,* Journal of the Acoustical Society of America 136(3), 1013-1028.